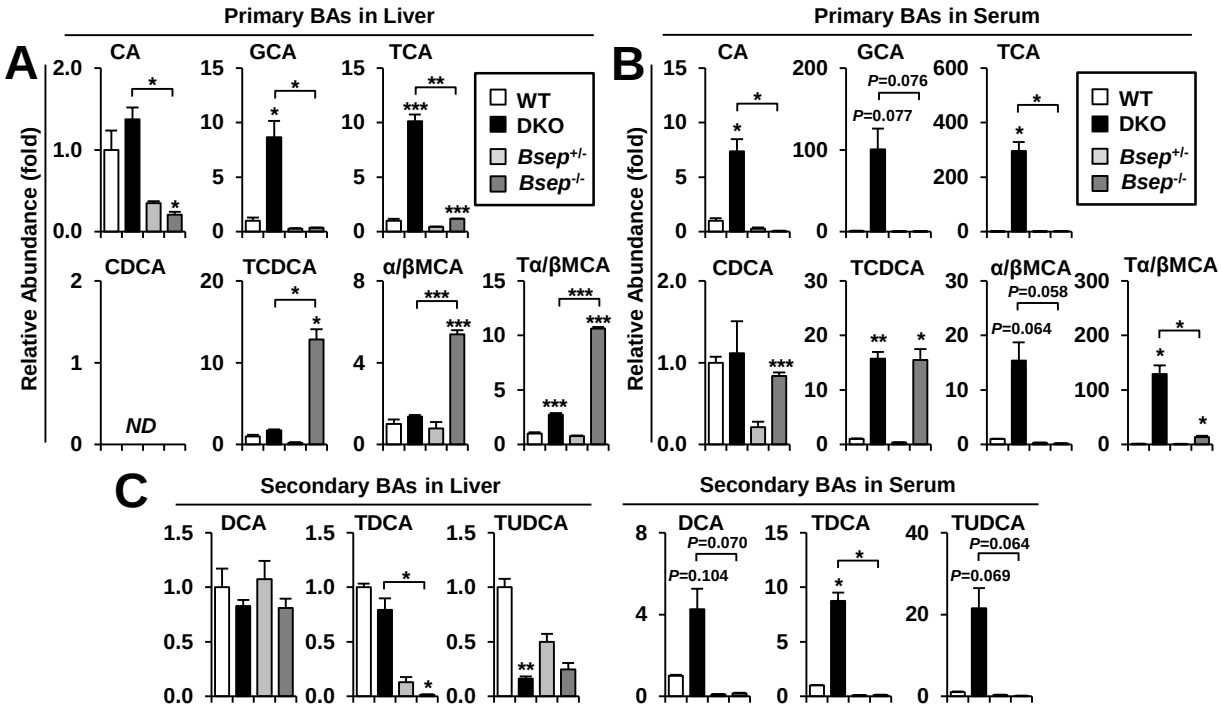

Supplemental Fig. S1

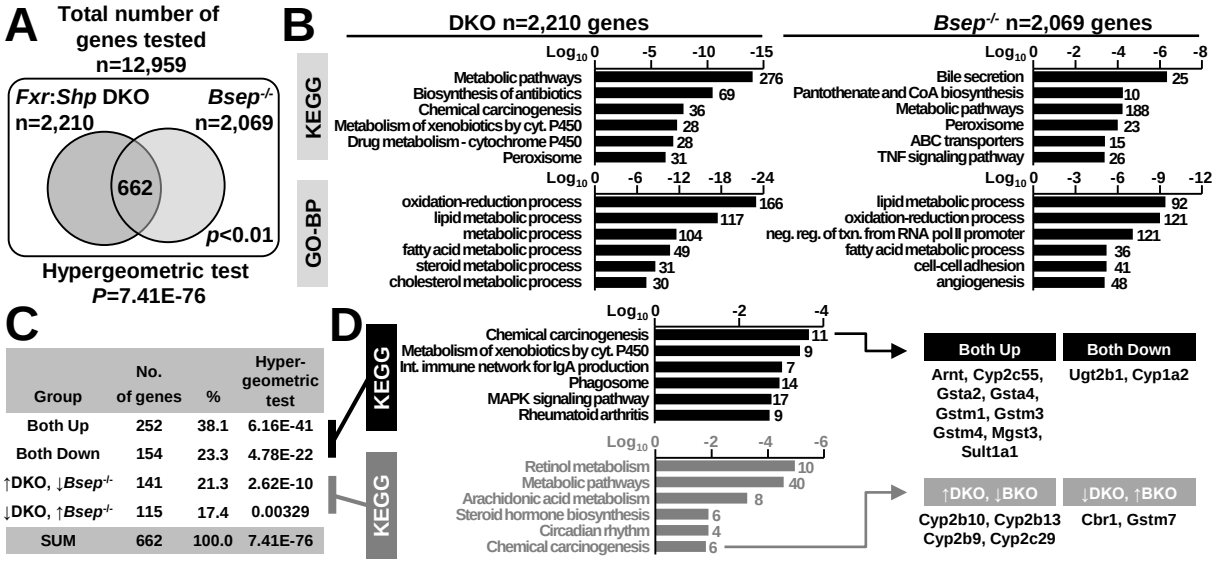

Supplemental Fig. S2

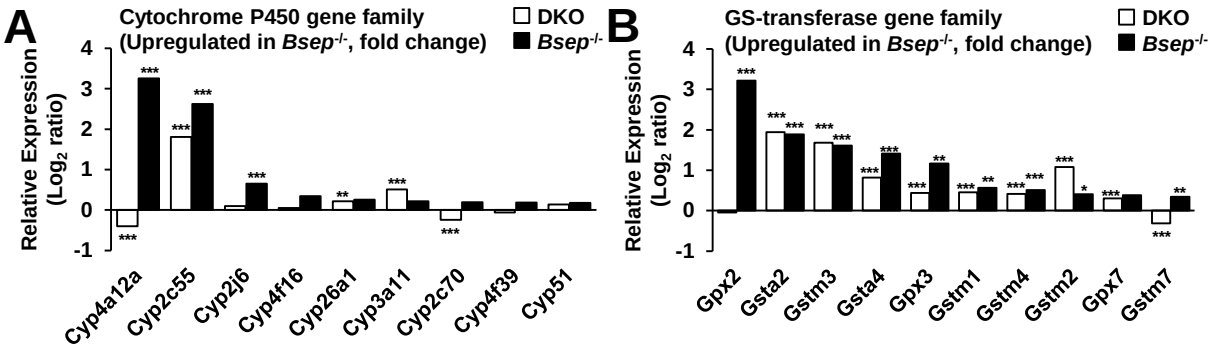

Supplemental Fig. S3

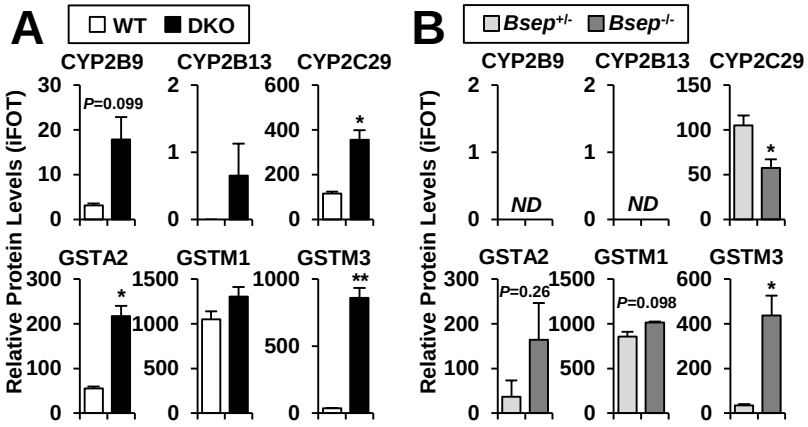

Supplemental Fig. S4

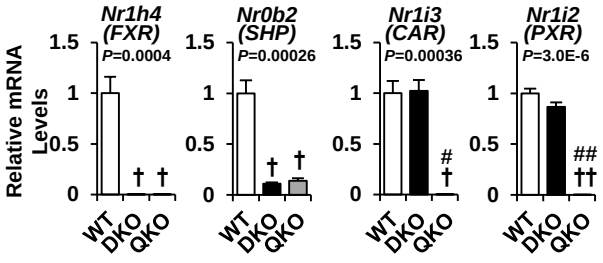

Supplemental Fig. S5

Normal human liver, CYP2B6, HPA048124

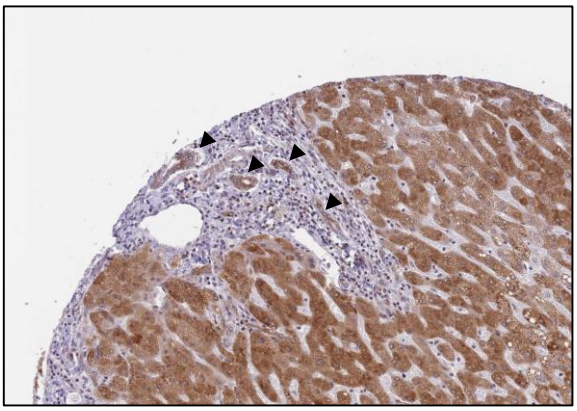

Supplemental Fig. S6

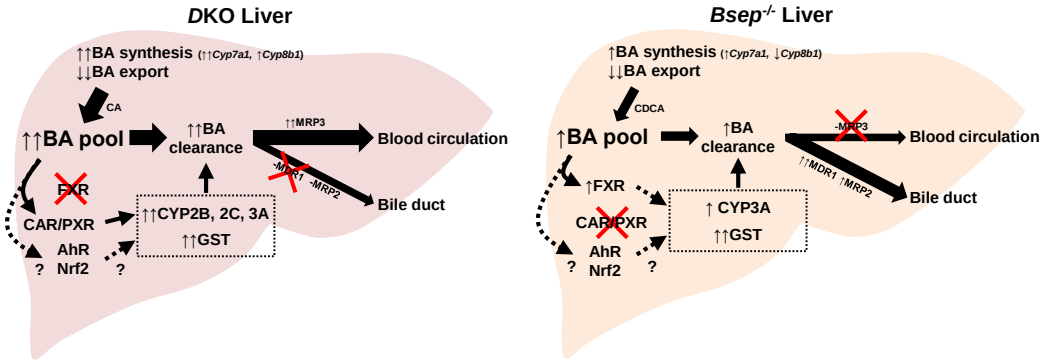

Supplemental Fig. S7

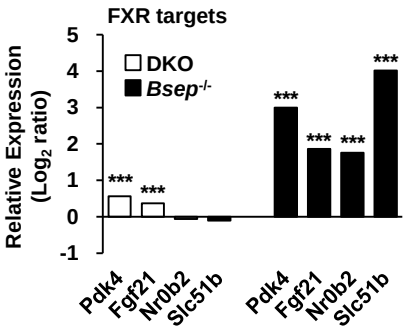

Supplemental Fig. S8

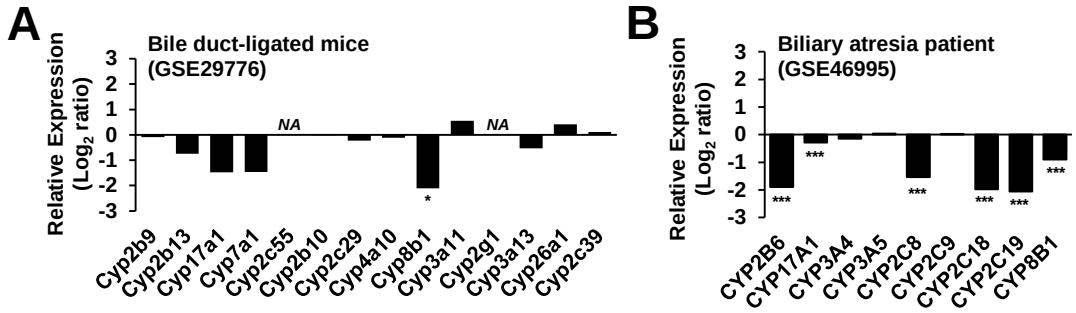

Supplemental Fig. S9

Supplemental Figure Legends

Supplemental Fig. S1. Comparison of relative BA levels in DKO and *Bsep*$^{-/-}$ liver and serum. Relative concentrations of (A, B) primary BAs and (C) secondary BAs were analyzed in liver and serum using UHPLC-MS-based metabolomics (n=3/each group). Area of each BA peak was normalized to WT control. Statistics: Student *t* test: **P*<0.05, ***P*<0.01, ****P*<0.005. In some cases, actual *P* value was presented. Abbreviation: ND, not detected.

Supplemental Fig. S2. KEGG pathway and Gene Ontology (Biological Pathway) analysis of altered gene lists in DKO and *Bsep*$^{-/-}$ microarray. (A) Among 12,959 genes, DKO and *Bsep*$^{-/-}$ exhibited 2,210 and 2,069 differentially-regulated genes, respectively (P<0.01). The 662 genes were overlapping. (B) Representative KEGG and Gene Ontology analysis results were shown (Supplemental Table S4 and S5). The number indicates the total gene number in each group. (C) Further categorization of overlapping 662 genes according to increased/decreased pattern. (D) Both up or downregulated 406 genes in DKO and *Bsep*$^{-/-}$ microarrays and 256 oppositely regulated genes were separately analyzed by DAVID Tools (Supplemental Table S4 and S5). The number indicates the total gene number in each group. Gene name belongs to chemical carcinogenesis was listed.

Supplemental Fig. S3. Cytochrome P450 genes are differentially regulated in DKO and *Bsep*$^{-/-}$. (A) Cytochrome P450 and (B) glutathione S-transferase genes were selected by the order of fold change in *Bsep*$^{-/-}$ microarray. The *P* value of each microarray was indicated with **P*<0.05, ***P*<0.01, ****P*<0.005.

Supplemental Fig. S4. Protein levels of cytochrome P450 genes and glutathione S-transferase gene. (A) Protein levels of representative CYP2B/2C and (B) Glutatione S-transferases were analyzed. Relative protein levels are indicated as intensity-based fraction of total (iFOT). Statistics: Student *t* test: **P*<0.05 and ***P*<0.01 compared to each control. In some cases, actual *P* value was presented.

Supplemental Fig. S5. Validation of nuclear receptor expressions in DKO and QKO. The *Fxr* (*Nr1h4*), *Shp* (*Nr0b2*), *Car* (*Nr1i3*), and *Pxr* (*Nr1i2*) expressions were analyzed by Q-PCR. Statistics: *P* values of one-way ANOVA test were indicated. *Post hoc t* test with Bonferroni correction: †,#*P*<0.0167, ††,##*P*<0.00333; †, compared to WT; #, compared to DKO.

Supplemental Fig. S6. Immunohistochemical analysis of CYP2B6 in normal human liver. CYP2B6 was highly detected in the hepatocytes as well as biliary epithelial cells (arrowhead). Image was downloaded from ProteinAtlas database (https://www.proteinatlas.org/ENSG00000197408-CYP2B6/tissue/liver#img).

Supplemental Fig. S7. Proposed model of DKO and *Bsep*$^{-/-}$ pathogenesis. In DKO liver, increased BA synthesis and decreased BA export causes BA accumulation that activates CAR/PXR signaling to compensate BA and bilirubin-induced hepatotoxicity through upregulation of cytochrome P450 and glutathione S-transferase expressions. Also, activated basolateral transporter accelerates BA efflux through blood circulation in DKO (MRP3). In *Bsep*$^{-/-}$ liver, increased hepatic BAs potentially activate FXR but not CAR/PXR. Inductions of canalicular transporters partially restore hepato-biliary BA circulation in *Bsep*$^{-/-}$.

Supplemental Fig. S8. Increase of known FXR target genes in *Bsep*$^{-/-}$. Gene expression of known FXR targets were analyzed in DKO and *Bsep*$^{-/-}$ microarrays. ***P<0.005.

Supplemental Fig. S9. Expressions of cytochrome P450 genes in bile duct-ligated mice or biliary atresia patients. Two microarrays ((A) GSE29776 and (B) GSE46995) was analyzed by GEO2R. Increase cytochrome P450 genes in DKO were listed. *P<0.05, ***P<0.005.

Supplemental Experimental Procedures

Detailed procedure of BA profiling by UHPLC-MS

Twenty microliters of serum were added to 60 μL of acetonitrile (1% NH4OH) including of LCA-D5 as the internal standard, followed by vortexing and centrifugation at 15,000 g for 15 min. Each supernatant was transferred to a sample vial for analysis. The liver was weighed and homogenized in 6 times volume of aqueous methanol (water: methanol 1:1 v/v) (100 mg of tissues in 600 μL of aqueous methanol). Then 100 μL of each mixture was added to 300 μL of acetonitrile (1% NH4OH *v/v*) including of LCA-D5 as the internal standard, followed by vortexing and centrifugation at 15,000 g for 15 min. The supernatant was transferred to a new Eppendorf vial for second centrifugation at 15,000 g for 15 min. Each supernatant was transferred to a sample vial for analysis.

Five microliters of the supernatant were injected into a liquid chromatography-tandem mass spectrometry (LC-MS/MS) for analysis (Agilent Technologies, 6490 QQQ Santa Clara, CA). Bile acid separation was achieved using a 1260 Infinity Binary LC System (Agilent Technologies, Santa Clara, CA) equipped with a 100 × 2.1 mm (Waters BEH C18) column. The column temperature was maintained at 45°C. The flow rate of was 0.2 mL/min with a gradient in a 25-min run. Gradients were run starting from 95% buffer A (H2O: Methanol, 80:20, *v/v*, pH 8.4) to 25% buffer B (CH3CN/H2O, 90:10 *v/v*, pH 8.4) from 0–5.0 min; 75% buffer A to 40% buffer B from 5.0-10.5 min; 60% buffer A to 95% buffer B from 10.5-18 min; 95% buffer B was held for 5 min; 95% B to 95% A from 23-23.5 min and held from 23.5-25 min to re-equilibrate the column. LC-MS/MS was operated in negative mode with electrospray ionization. Ultra-highly pure nitrogen was applied as the drying gas and the collision gas.

Detailed procedure of proteome profiling by LC-MS/MS

Frozen mice liver tissue was homogenized by cryogenic grinding, dispersed by pipetting in 10 sample volume of lysis buffer (50 mM ammonium bicarbonate, 1 mM $CaCl_2$) and then snap frozen using liquid nitrogen and thawed at 37°C twice. Proteins were then boiled at 95°C for 3 min. All freeze-thaw-denaturation procedures were repeated three times. The 50 μg of denatured protein was digested twice with 1ug of trypsin (GenDEPOT, T9600) overnight and 500 ng for 4 h at 37°C. Double-digested peptides were extracted by 50% Acetonitrile/0.1% formic acid and peptide supernatant was taken after spin-down at 10,000 g for 1 min. The remaining pellet was extracted with 80% acetonitrile/0.1% formic acid once again and pooled into previous extract after spin down. Pooled peptide supernatant was quantified again using colorimetric method (Pierce™ Quantitative Colorimetric Peptide Assay, Thermo Fisher Scientific). The 50 μg of peptide was taken and dried using vacuum drier. Vacuum dried peptides were fractionated as previously described.(17) Briefly, peptide was dissolved in pH 10 (10 mM ammonium bicarbonate, pH adjusted by NH_4OH) buffer and subjected to pH 10 C18 reverse phase column chromatography. A micro pipet tip C18 column was made from 200 μL pipet tip by layering 6 mg of C18 matrix (Reprosil-Pur Basic C18, 3 μm) on top of the C18 disk (3M, Empore ™ C18) plug. Peptides in pH 10 buffer were loaded on the C18 tip equilibrated with pH10 solution then washed with pH10 buffer twice. Bounded peptide was eluted with step gradient of 150 μL of 6, 9, 12, 15, 18, 21, 25, 30, 35% ACN (pH 10) and pooled into 6 pools (6% eluent combined with 25% eluent, 9% plus 30%, and 12% plus 35%) and vacuum dried for nanoHPLC-MS/MS. Vacuum dried peptide was dissolved in 40 μL of loading solution (5% methanol containing 0.1% formic acid) and 5 μL of the reconstituted samples were subjected to nanoLC-MS/MS analysis with a nano-LC 1000 (Thermo Fisher Scientific) coupled to Thermo

Q-Exactive (Thermo Fisher Scientific) mass spectrometer. The peptides were loaded onto an in-house Reprosil-Pur Basic C18 (3 μm, Dr.Maisch GmbH, Germany) trap column that was 2 cm x 100 μm size. Then the trap column was washed with loading solution and switched in-line with an in-house 5 cm x 150 um column packed with Reprosil-Pur Basic C18 equilibrated in 0.1% formic acid/water. The peptides were separated with 75 min discontinuous gradient of 2-24, 4-24 or 8-26% acetonitrile/0.1% formic acid at a flow rate of 800 nL/min. Separated peptides were directly electro-sprayed into mass spectrometer. The instrument was operated in data-dependent mode, acquiring fragmentation spectra of the top 35 strongest ions and under direct control of Xcalibur software (Thermo Fisher Scientific). Parent MS spectrum and HCD fragmented MS/MS spectrum were acquired in the Orbitrap with resolution of 140,000 and 17,500. The full MS range was 375-1300 m/z and the trap target was 3,000,000 and 20,000. Obtained MS/MS spectra were searched against target-decoy Mouse refseq database (release 2015_06, containing 58549 entries) in Proteome Discoverer 1.4 interface (PD1.4, Thermo Fisher Scientific) with Mascot algorithm (Mascot 2.4, Matrix Science). Variable modification of Oxidation of methionine was allowed. The precursor mass tolerance was confined within 20 ppm with fragment mass tolerance of 0.02 Dalton and a maximum of two missed cleavages was allowed. Assigned peptides were filtered with 1% false discovery rate (FDR) and subject to manual verifications. AUC-based relative quantification was analyzed by iBAQ algorithm and normalized to iFOT to compare protein levels (17).

17. Jung SY, Choi JM, Rousseaux MW, Malovannaya A, Kim JJ, Kutzera J, Wang Y, et al. An Anatomically Resolved Mouse Brain Proteome Reveals Parkinson Disease-relevant Pathways. Mol Cell Proteomics 2017;16:581-593.

Supplemental Tables

Supplemental Table S1. Primer sequences used for Q-PCR

Gene symbol	Forward primer	Reverse primer
Gapdh	CTTTGGCATTGTGGAAGGGC	CAGGGATGATGTTCTGGGCA
Cyp7a1	CTGGGGGATTGCTGTGGTAG	GCACAGCCCAGGTATGGAAT
Cyp8b1	TTGCAAATGCTGCCTCAACC	TAACAGTCGCACACATGGCT
Cyp7b1	CTCTTTGCCGCCACCTTACT	ATCAAGGGTGGTTCACGAGG
Cyp27a1	GGCAAGTACCCAATAAGAGACCA	AAAGCCTGACGCAGATGGTA
Cyp2b10	AGTGGAGGAACTGCGGAAATC	AGCAGGCGCAAGAACTGAC
Cyp3a11	AAACTGCAGGATGAGATCGAT	TCCAGGTATTCCATCTGCATC
Ugt1a1	CCTTCTGTTGTGTGTGTTCGG	CTGCTGGAGCTGCTGAATAAC
Sult2a1	CCTCAAAGGAAATGTTCTATTCGGA	CCATTCTCTCATGGACAGCCA
Abcb11	GCTGCCAAGGATGCTAATGC	CTACCCTTTGCTTCTGCCCA
Abcb1a	CAGCAGTCAGTGTGCTTACA	CATCATAAGTGGGAGCGCCA
Abcc2	CGTAACAGAAGTGCCCTGGA	GTCGGCTTCCGGACTTTTCA
Abcg2	AAACTTGCTCGGGAACCCTC	TGCATTCCAGCGGCATCATA
Abcc3	ACTGCACCGTACTGACCATC	CCGCAATGAGGTTGACTGGA
Abcc4	GAGCACACGGACGAGGAG	TCTTCAATGGCCTCTTTAAGTTG
Slc51a	GAAAGAGGTGGAAGGGACCG	CTCCTCAAGCCTCCAGTGTC
Slc51b	CAGAGAAACCAGACTTGGCCC	GGGCGTTATGGGGTACTCTC
Slc10a1	TTCACTGGCTTCCTGATGGG	CTGTTTCCATGCTGATGGTGC
Oatp1b2	CTTGGGTTGTCGGTGGAAGG	TGGATGCTGAGTTTGGTCCAT
Abcb4	CGGCGACTTTGAACTAGGCA	GCCAGTCAGAGTATCGGAACA
Atp8b1	ACAAGAAAGCCATCACCCTGG	ATGACAGCTTGCATCCCTTCT
Nr1h4	TCCGGACATTCAACCATCAC	TCACTGCACATCCCAGATCTC
Nr0b2	CGATCCTCTTCAACCCAGATG	AGGGCTCCAAGACTTCACACA
Nr1i3	GCTGCAAGGGCTTCTTCAG	AACGGACAGATGGGACCAA
Nr1i2	CAAGGCCAATGGCTACCA	CGGGTGATCTCGCAGGTT
Cyp2b9	TGGAACTGAGACCACAAGCG	AAGAGTTGGTAGCCGGTGTG
Cyp2b13	TTCTCCACAGCTGGAAGGTG	CCAGAAGTCTCTGTTCACAAATCAAG
Cyp2c29	GGGCTCAAAGCCTACTGTCAT	TCGTCTCATCTCTTTCCATCTG
Cyp4a10	AACAGAAGAGTGGATGAACTATGAGT	GCCATTGCCTGTGGAGGTAG
Cyp17a1	ATCAGCTGGCCAGAGAAGTG	TACTATCCGCAAAGGCGACG
Gsta2	GGAAGGTTTTCAAGTTTTAGTGTGG	CACAATAGCCAGAATCAACAATTGTA
Gstm1	ATGTTTGAGCCCAAGTGCCT	TAGGTGTTGCGATGTAGCGG
Gstm2	GAGGAGAGGATTCGTGTGGAC	TCATCTTCTCAGGGAGACCC
Gstm3	CACAACCTGTGTGGAGAGACA	GGGACTGCAGCAGACTATCAT
Gstt3	TGCCGTGCTGTCTACATCTTC	TGGGCGAAGGAATCTGTGTA

Supplemental Table S2. Expression profile of genes involved in BA homeostasis

Function	Gene	DKO		*Bsep*$^{-/-}$	
		Fold change	***P* value**	**Fold change**	***P* value**
BA synthesis	CYP7A1	5.047	0.0038	1.143	0.5400
	CYP8B1	3.238	0.0088	0.252	0.1486
	CYP7B1	0.049	0.0054	0.123	0.0088
	Cyp27A1	0.597	0.0014	1.152	0.1371
BA metabolism	CYP2B10	29.636	0.0180	2.376	0.2689
	CYP3A11	21.524	P<0.0001	8.154	0.0215
	UGT1A1	1.567	0.0257	1.441	0.0230
	SULT2A1	4.340	0.1209	0.445	0.3959
BA transport into bile duct	ABCB11 (BSEP)	0.162	P<0.0001	6.6E-06	0.0099
	ABCB1A (MDR1A)	3.696	0.0095	17.782	0.0569
	ABCC2 (MRP2)	1.357	0.0019	1.124	0.3738
	ABCG2 (BCRP)	1.035	0.5879	0.933	0.6681
BA transport into circulation	ABCC3 (MRP3)	3.497	0.0013	1.860	0.0176
	ABCC4 (MRP4)	19.985	0.0284	4.957	0.0953
	SLC51A (OST-A)	1.122	0.5997	1.136	0.8592
	SLC51B (OST-B)	0.059	0.0796	20.353	0.0593
BA uptake	SLC10A1 (NTCP)	0.390	0.0547	1.008	0.9471
	OATP1B2 (OATP1)	0.638	0.0226	0.859	0.2458
Other PFIC genes	ABCB4 (MDR2)	0.855	0.1291	1.821	0.0054
	ATP8B1 (FIC1)	0.478	0.0216	1.151	0.2511
Nuclear receptors	NR1H4 (FXR)	4.99E-05	0.0043	0.771	0.0844
	NR0B2 (SHP)	0.002	0.0187	1.845	0.0533
	NR1I3 (CAR)	0.657	0.0129	0.996	0.9782
	NR1I2 (PXR)	0.791	0.1856	1.679	0.0447

Notes: The mRNA expression profile in 3 months-old DKO and *Bsep*$^{-/-}$ (n=3/group) analyzed by Q-PCR. In addition to the official gene symbol, common gene name was given in parentheses.

Supplemental Table S3. Proteomic analysis of DKO and *Bsep*$^{-/-}$ liver

Function	Gene	DKO				*Bsep*$^{-/-}$			
		WT (iFOT)	DKO (iFOT)	Fold change	*P* value	*Bsep*$^{+/-}$ (iFOT)	*Bsep*$^{-/-}$ (iFOT)	Fold change	*P* value
BA synthesis	CYP7A1	0.01	3.93	295.00	0.0098	0.11	0.81	7.33	0.0008
	CYP8B1	5.80	34.47	5.94	0.0050	7.33	0.32	0.04	0.0211
	CYP7B1	23.20	3.93	0.17	0.0058	14.23	3.90	0.27	0.2171
	Cyp27A1	39.03	22.93	0.59	0.0011	46.97	35.60	0.76	0.0644
BA metabolism	CYP2B10	1.29	20.93	16.27	0.0724	ND			
	CYP3A11	27.27	653.00	23.95	0.0018	30.60	155.67	5.09	0.0096
	UGT1A1	114.53	173.33	1.51	0.2868	185.00	143.67	0.78	0.3581
	SULT2A1	9.00	67.43	7.49	0.1858	22.53	7.80	0.35	0.0822
BA transport into bile duct	ABCB11 (BSEP)	3.20	0.50	0.16	0.0230	4.30	0.00	0.00	0.0651
	ABCB1A (MDR1A)	ND				ND	0.60	NA	0.0248
	ABCC2 (MRP2)	1.20	1.05	0.87	0.6904	1.53	3.10	2.03	0.0383
	ABCG2 (BCRP)	1.24	0.74	0.59	0.2436	0.72	0.97	1.34	0.3837
BA transport into circulation	ABCC3 (MRP3)	0.18	1.38	7.65	0.0751	0.09	0.14	1.56	0.4015
	ABCC4 (MRP4)	0.14	0.06	0.43	0.2891	0.07	0.06	0.86	0.8327
	SLC51A (OST-A)	ND				ND			
	SLC51B (OST-B)	ND				ND			
BA uptake	SLC10A1 (NTCP)	8.90	2.30	0.26	0.0691	6.13	6.63	1.08	0.7903
	OATP1B2 (OATP1)	ND				ND			
Other PFIC genes	ABCB4 (MDR2)	1.08	1.01	0.94	0.9204	0.24	1.80	7.38	0.0719
	ATP8B1 (FIC1)	0.16	0.00	0.00	0.4226	ND			

Notes: Total proteome in DKO and *Bsep*$^{-/-}$ liver (n=3/group). Relative protein levels are indicated as intensity-based fraction of total (iFOT). In addition to the official gene symbol, some common gene names are in parentheses.
Abbreviations: ND, not detected; NA, not applicable; iFOT, intensity-based fraction of total.

Supplemental Table S4. DAVID analysis of KEGG pathway

Category	Term	Count	%	P-Value	Benjamini
DKO (Supplemental Fig. S2B)					
KEGG_PATHWAY	Metabolic pathways	276	12.5	9.70E-15	2.80E-12
KEGG_PATHWAY	Biosynthesis of antibiotics	69	3.1	3.30E-11	4.80E-09
KEGG_PATHWAY	Chemical carcinogenesis	36	1.6	1.30E-08	1.30E-06
KEGG_PATHWAY	Metabolism of xenobiotics by cytochrome P450	28	1.3	4.80E-08	3.50E-06
KEGG_PATHWAY	Drug metabolism - cytochrome P450	28	1.3	1.10E-07	6.10E-06
KEGG_PATHWAY	Peroxisome	31	1.4	5.30E-07	2.60E-05
KEGG_PATHWAY	Carbon metabolism	36	1.6	7.80E-06	3.20E-04
KEGG_PATHWAY	Retinol metabolism	30	1.4	9.00E-06	3.20E-04
KEGG_PATHWAY	Glycine, serine and threonine metabolism	18	0.8	1.30E-05	4.30E-04
KEGG_PATHWAY	Biosynthesis of amino acids	27	1.2	1.60E-05	4.70E-04
KEGG_PATHWAY	Complement and coagulation cascades	25	1.1	9.20E-05	2.40E-03
KEGG_PATHWAY	Glutathione metabolism	20	0.9	1.30E-04	3.10E-03
KEGG_PATHWAY	Bile secretion	23	1	2.40E-04	5.40E-03
KEGG_PATHWAY	Amino sugar and nucleotide sugar metabolism	18	0.8	2.70E-04	5.60E-03
KEGG_PATHWAY	Steroid hormone biosynthesis	26	1.2	3.50E-04	6.70E-03
KEGG_PATHWAY	Valine, leucine and isoleucine degradation	19	0.9	4.20E-04	7.50E-03
KEGG_PATHWAY	Glucagon signaling pathway	28	1.3	6.20E-04	1.00E-02
KEGG_PATHWAY	Fatty acid degradation	17	0.8	8.90E-04	1.40E-02
Bsep$^{-/-}$ (Supplemental Fig. S2B)					
KEGG_PATHWAY	Bile secretion	25	1.2	4.60E-07	1.30E-04
KEGG_PATHWAY	Pantothenate and CoA biosynthesis	10	0.5	5.80E-05	8.10E-03
KEGG_PATHWAY	Metabolic pathways	188	9.1	6.00E-05	5.70E-03
KEGG_PATHWAY	Peroxisome	23	1.1	1.00E-04	7.20E-03
KEGG_PATHWAY	ABC transporters	15	0.7	4.00E-04	2.20E-02
KEGG_PATHWAY	TNF signaling pathway	26	1.3	4.20E-04	2.00E-02
KEGG_PATHWAY	Steroid hormone biosynthesis	22	1.1	5.90E-04	2.30E-02
Both Up/Down (Supplemental Fig. S2D)					
KEGG_PATHWAY	Chemical carcinogenesis	11	0	2.20E-04	4.70E-02
KEGG_PATHWAY	Metabolism of xenobiotics by cytochrome P450	9	0	3.60E-04	3.90E-02
KEGG_PATHWAY	Intestinal immune network for IgA production	7	0	9.60E-04	6.90E-02
KEGG_PATHWAY	Phagosome	14	0	1.10E-03	5.70E-02
KEGG_PATHWAY	MAPK signaling pathway	17	0	1.70E-03	7.50E-02
KEGG_PATHWAY	Rheumatoid arthritis	9	0	1.90E-03	6.80E-02
KEGG_PATHWAY	Peroxisome	9	0	2.00E-03	6.30E-02
KEGG_PATHWAY	Drug metabolism - cytochrome P450	8	0	2.20E-03	6.00E-02
Opposite regulation (Supplemental Fig. S2D)					
KEGG_PATHWAY	Retinol metabolism	10	0	1.10E-05	2.30E-03
KEGG_PATHWAY	Metabolic pathways	40	0.1	2.70E-05	2.70E-03
KEGG_PATHWAY	Arachidonic acid metabolism	8	0	5.40E-04	3.50E-02
KEGG_PATHWAY	Steroid hormone biosynthesis	6	0	1.30E-02	4.70E-01
KEGG_PATHWAY	Circadian rhythm	4	0	1.30E-02	4.10E-01
KEGG_PATHWAY	Chemical carcinogenesis	6	0	1.60E-02	4.10E-01
KEGG_PATHWAY	Bile secretion	5	0	2.70E-02	5.40E-01
KEGG_PATHWAY	Sphingolipid metabolism	4	0	4.10E-02	6.50E-01

Supplemental Table S5. DAVID analysis of Gene Ontology (Biological Pathways)

Category	Term	Count	%	P-Value	Benjamini
DKO (Supplemental Fig. S2B)					
GOTERM_BP_DIRECT	oxidation-reduction process	166	7.5	1.10E-23	5.80E-20
GOTERM_BP_DIRECT	lipid metabolic process	117	5.3	3.20E-18	8.80E-15
GOTERM_BP_DIRECT	metabolic process	104	4.7	2.50E-12	4.50E-09
GOTERM_BP_DIRECT	fatty acid metabolic process	49	2.2	2.10E-11	2.90E-08
GOTERM_BP_DIRECT	steroid metabolic process	31	1.4	2.40E-09	2.60E-06
GOTERM_BP_DIRECT	cholesterol metabolic process	30	1.4	4.70E-08	4.30E-05
GOTERM_BP_DIRECT	glutathione metabolic process	21	1	8.50E-08	6.60E-05
GOTERM_BP_DIRECT	response to drug	72	3.3	8.50E-08	5.80E-05
GOTERM_BP_DIRECT	response to lipopolysaccharide	47	2.1	6.80E-07	4.10E-04
GOTERM_BP_DIRECT	positive regulation of apoptotic process	67	3	2.30E-06	1.30E-03
GOTERM_BP_DIRECT	gluconeogenesis	13	0.6	7.30E-06	3.60E-03
GOTERM_BP_DIRECT	fatty acid beta-oxidation	17	0.8	9.90E-06	4.50E-03
GOTERM_BP_DIRECT	autophagy	35	1.6	1.00E-05	4.40E-03
GOTERM_BP_DIRECT	response to hypoxia	43	2	1.20E-05	4.50E-03
GOTERM_BP_DIRECT	sterol biosynthetic process	13	0.6	1.20E-05	4.30E-03
GOTERM_BP_DIRECT	lipid homeostasis	16	0.7	1.70E-05	5.80E-03
GOTERM_BP_DIRECT	immune system process	71	3.2	1.70E-05	5.60E-03
GOTERM_BP_DIRECT	aging	39	1.8	2.70E-05	8.20E-03
GOTERM_BP_DIRECT	liver development	26	1.2	2.80E-05	7.90E-03
GOTERM_BP_DIRECT	apoptotic process	96	4.4	3.10E-05	8.30E-03
GOTERM_BP_DIRECT	endoplasmic reticulum unfolded protein response	17	0.8	3.50E-05	8.90E-03
GOTERM_BP_DIRECT	retinoic acid metabolic process	9	0.4	7.10E-05	1.70E-02
GOTERM_BP_DIRECT	cholesterol biosynthetic process	13	0.6	9.00E-05	2.10E-02
Bsep$^{-/-}$ (Supplemental Fig. S2B)					
GOTERM_BP_DIRECT	lipid metabolic process	92	4.5	4.10E-10	2.10E-06
GOTERM_BP_DIRECT	oxidation-reduction process	121	5.9	1.00E-09	2.60E-06
GOTERM_BP_DIRECT	negative regulation of transcription from RNA polymerase II promoter	121	5.9	8.70E-08	1.50E-04
GOTERM_BP_DIRECT	fatty acid metabolic process	36	1.7	6.20E-06	8.10E-03
GOTERM_BP_DIRECT	cell-cell adhesion	41	2	6.40E-06	6.70E-03
GOTERM_BP_DIRECT	angiogenesis	48	2.3	8.60E-06	7.50E-03
GOTERM_BP_DIRECT	phosphorylation	95	4.6	3.90E-05	2.90E-02
GOTERM_BP_DIRECT	apoptotic process	89	4.3	5.60E-05	3.60E-02
GOTERM_BP_DIRECT	steroid metabolic process	22	1.1	8.40E-05	4.80E-02
Both Up/Down (Supplemental Fig. S1D)					
GOTERM_BP_DIRECT	angiogenesis	17	0	3.50E-05	6.80E-02
GOTERM_BP_DIRECT	steroid metabolic process	10	0	5.40E-05	5.30E-02
GOTERM_BP_DIRECT	antigen processing and presentation of exogenous peptide antigen via MHC class II	5	0	1.50E-04	9.30E-02
GOTERM_BP_DIRECT	oxidation-reduction process	30	0.1	1.50E-04	7.20E-02
GOTERM_BP_DIRECT	positive regulation of fibroblast proliferation	8	0	3.60E-04	1.30E-01
GOTERM_BP_DIRECT	circadian rhythm	10	0	3.80E-04	1.20E-01
GOTERM_BP_DIRECT	metabolic process	22	0	6.00E-04	1.60E-01
GOTERM_BP_DIRECT	response to drug	18	0	6.50E-04	1.50E-01
GOTERM_BP_DIRECT	antigen processing and presentation of peptide or polysaccharide antigen via MHC class II	4	0	6.50E-04	1.30E-01
GOTERM_BP_DIRECT	inflammatory response	18	0	7.60E-04	1.40E-01
Opposite regulation (Supplemental Fig. S2D)					
GOTERM_BP_DIRECT	oxidation-reduction process	27	0.1	7.40E-07	1.10E-03
GOTERM_BP_DIRECT	lipid metabolic process	20	0.1	8.90E-06	6.70E-03
GOTERM_BP_DIRECT	fatty acid metabolic process	9	0	9.80E-04	3.90E-01

GOTERM_BP_DIRECT	response to peptide hormone	6	0	2.60E-03	6.20E-01
GOTERM_BP_DIRECT	regulation of glucose metabolic process	4	0	4.00E-03	7.00E-01
GOTERM_BP_DIRECT	positive regulation of cell adhesion	5	0	5.90E-03	7.80E-01
GOTERM_BP_DIRECT	epoxygenase P450 pathway	4	0	6.70E-03	7.70E-01